Natural Hazards (2022) 112:697–723
https://doi.org/10.1007/s11069-021-05201-x

ORIGINAL PAPER

Appraisal of seasonal drought characteristics in Turkey during 1925–2016 with the standardized precipitation index and copula approach

Emre Topçu[1]

Received: 25 May 2021 / Accepted: 29 December 2021 / Published online: 7 January 2022
© The Author(s), under exclusive licence to Springer Nature B.V. 2022

Abstract
Drought is caused by the imbalances in the factors that make up the hydrological cycle, especially the rainfall. Droughts triggered by climate change can occur anywhere in the world. This study aims to conduct a detailed seasonal drought analysis through the monthly precipitation statistics of 126 observational points in Turkey during 1925–2016. The drought analysis was performed for four different periods: 1925–1949, 1950–1974, 1975–1999, and 2000–2016. First, the standardized precipitation index values were calculated with the Pearson Type III distribution. The 3-month period, used in seasonal drought analysis, was preferred. Information about the course of drought was obtained with the Mann–Kendall trend analysis. The severity, duration, and frequency of drought were found with the Theory of Runs model. The joint return period of drought severity and drought duration were obtained with the copula approach. The mapping was done with the inverse distance weighted method. The findings indicate that the lowest SPI value (− 2.12) was observed in spring 1972 and the highest SPI value (2.14) was observed in winter 1941. Very dry conditions were recorded with a frequency of 16% in the spring season of the 1925–1949 period; the most normal arid conditions were documented in the autumn season of 1950–1974 with a frequency of 52%. Extreme drought conditions were reported in the spring season in 1992. While there was an insignificant increase in drought in spring, summer, and winter, a significant increase was observed in autumn especially interior parts of Turkey. Theory of Runs results indicate that the highest intensity, with a value over 2, was observed in the southeast of Turkey during the winter and spring seasons during the 1925–2016 period. The Frank copula function was found to be the most suitable function in calculations of the drought severity and duration calculation for Turkey. The return periods of weak, moderate, and severe droughts were between 127.53 and 78.96, 68.85 and 59.60, 60.28 and 57.65 months, respectively. It was determined that the drought severity increased in the inner regions during the 20- and 100-year drought return periods with the values varying between 5 and 16, 7, and 32, respectively.

Keywords Copula · Drought · Mann–Kendall · Standardized precipitation index · Theory of Runs · Turkey

✉ Emre Topçu
emretopcu01@gmail.com

[1] Civil Engineering Department, Kafkas University, 36100 Kars, Turkey

1 Introduction

Shortage of water is mainly defined as drought, a condition in which the water is not sufficient to meet natural survival or economical activity. Droughts have become a climate phenomenon that is more frequently emphasized with global warming (Mishra and Singh 2010; Yu et al. 2014; An et al. 2020).

The changing global energy balance has altered the patterns of the atmospheric variables as a result of warming. The occurrence of droughts, and their frequency and severity in many regions, are triggered by the increase in global temperature. The main response to changes in drought patterns is the availability of water, which is a significant factor for food security, agricultural productivity, and water stress. Droughts are exceptional once compared with other natural disasters, as they emerge slowly and have higher longevity. Defining drought arrival, duration, and the end is ambiguous as its effects only appear gradually as agriculture is more drastically affected by drought than other natural disasters (Lake 2003; Samarah 2005; European Commission 2007; Wilhite et al. 2007; Farooq et al. 2009; Mishra and Singh 2011; Trenberth et al. 2014; Wilhite et al. 2014; Ahmed et al. 2016; Salman et al. 2017; Ahmed et al. 2018; 2019; Khan et al. 2019; Qutbudin 2019; Shiru et al. 2019).

The decrease in precipitation is the leading cause for prolonged drought periods. Incidentally, this is driven by global warming and climate change, caused by greenhouse gas (GHG) emissions (IPCC 2007; 2014). Water shortage, dwindling agricultural production, and surface flow declines are among the problematic products of overlong drought periods (Seckler et al. 1999; Mancosu et al. 2015). Distinguishing their commencement, frequency, and severity is important to forecast and predict the characteristics of droughts. Besides the systematic evolution of climate phenomena, some other arbitrary elements affect numerous human activities. These elements include runoff and soil moisture which change the hydrological cycle and unforecastable precipitation. It is unclear that such alterations can be predicted through the probabilistic, statistical, and stochastic methodologies (Şen and Almazroui 2021). Depending on the physical impact on the environment, four categories of drought exist (Wilhite and Glantz 1985). These are namely meteorological, agricultural, hydrological, and socioeconomic drought (Addi et al. 2021).

Meteorological drought is solely pertinent to weather conditions; it is defined as lessening in the average amount of precipitations compared with at least the recorded 30 years of precipitation series. The other two types of drought are influenced by meteorological drought, and they come after it. Agricultural drought is caused by the scarcity of soil moisture that triggers wilting and plant death in agriculture. Agricultural drought could occur even though adequate precipitations and water resources. Too much water usage and unnecessary agricultural activities may cause the latter. The extent of the drought will be amplified with the moistureless winds. Hydrological drought happens when the precipitation and water in reservoirs are inadequate due to either dense population or high rural activities such as irrigation. Urban life encounters challenges during hydrological droughts, hydroelectric power production, and sprinkler systems get severely affected. This may lead to problems such as economic crisis or financial support shortages. It has been observed that soil moisture reduced very slowly in cases of dry weather longer than 2 weeks. The maximum evaporation rate rises in cases with longer duration leading to water reservoirs, including subsurface water. Hence, hydrologists term this type of drought as creeping phenomenon (Topçu and Seçkin 2016).

Continuous population growth and rapid economic development have dramatically increased global water consumption. This trend will most certainly continue in the near future (Chen et al. 2016; Shi et al. 2019) and possibly cause extra socioeconomic drought cases (Smirnov et al. 2016; Trinh et al. 2017; Liu et al. 2020).

Unbiased drought indices can be applied to drought features for comparing the temporal and spatial variation of historical droughts with the current conditions. Drought characteristics such as severity, maximum duration, and frequency of occurrence can also be quantified through drought indices. They also help decision-makers as a tool to assess drought cases and to plan mitigation to contain their impacts (Mishra and Singh 2010; Maccioni et al. 2015; Mahajan and Dodamani 2016; Gupta and Jain 2017; Singh et al. 2019).

Turkey is located in the East Mediterranean region. Through the influence of the Mediterranean depression, 67% of precipitation during the winter and spring months in Turkey with annual average precipitation of 630 mm (Türkeş 1996; Kömüşçü 2001; Sönmez et al. 2005). Europe is expected to face prolonged and more intensive droughts extending over larger areas in the Mediterranean region (Jones et al. 1996; Vicente-Serrano and Begueria 2006). Thus, monitoring and planning for its management have the highest importance for the Mediterranean region (Cavus and Aksoy 2019). Once the alteration in annual precipitation and winter season (high season for rain and snow in Turkey), 1971–1974, 1983–1984, 1989–1990, 1996–2001, and 2007–2008 emerges as the longest and most severe droughts in the past 40 years. The longest of these droughts began as meteorological droughts and later developed into agricultural and hydrological droughts (Kurnaz 2014).

Precipitation anomalies are a natural recurring characteristic of the global climate, and they affect different elements of the hydrological cycle to produce drought (Geiger 1954). However, a successful drought monitoring depends on how the drought is characterized and quantified not only for spatial but also for temporal extents (Musonda et al. 2020).

This study presents a seasonal (spring, summer, autumn, and winter) drought analysis performed meteorologically with the help of SPI method using monthly total precipitation data between the years 1925–2016 of 126 observational points in Turkey. The main purpose of the study is to follow how the seasonal drought changes over the specified periods through the SPI results. Therefore, the goal was to detect the drought trends and the severity and duration corresponding to certain recurrence periods in this study. The main findings were presented and discussed in the conclusion.

2 Materials and methods

2.1 Material

Hydrology, climatology, ecology, and agricultural models acquire their primary input data from one of the essential elements of the hydrologic cycle, namely, the precipitation (Guofeng et al. 2017). Thus these models' reliability relies on the accurateness and continuity of the precipitation data not only in temporal and spatial resolutions (Zhu et al. 2016) but also in areas with complex orography (Petracca et al. 2018). Despite its importance, precipitation data in Turkey are difficult to obtain accurately due to an inadequate number of current meteorological stations that are thinly and irregularly distributed over the country and mountainous regions in particular. Moreover, the majority of the stations are located in places such as cities and airports. Thus, these stations may not even accurately characterize their regions (Irvem and Ozbuldu 2019).

Ground observations, with their relatively higher accuracy and long-term records, are the components of conventional drought monitoring. Besides, they are not abundant in number or homogeneously spread. They are even unavailable for common users in most regions around the globe (Miao et al. 2015). Thus drought monitoring dependent on ground observations is bounded with disadvantages and limitations because they can only provide limited and variable representativeness. Although spatial interpolation possibly some of these problems, they will bring in extra uncertainty, especially in the regions with sparse and uneven instruments, such as mountains (Naumann et al. 2012; Kaptue et al. 2015; Guo et al. 2017).

Furthermore, more accurate and continuous observation data, that can be used to identify the areal precipitation distribution, can be acquired through satellite-based precipitation products for the whole globe (Irvem and Ozbuldu 2019).

This study used the monthly total precipitation (mm) during 1925–2016 as a meteorological parameter. All of the data are taken from the source (World Bank Climate Change Knowledge Portal 2021). The historical temperature and precipitation data generated from the 2-degree scored data by country and basin levels stored in this database. The meteorological data in this resource were obtained through the portal created in collaboration with The National Center for Atmospheric Research (NCAR), The International Research Institute (University of Columbia), and The European Space Agency (ESA) Earth Observation for Sustainable Development (EO4SD) initiative. The National Center for Atmospheric Research (NCAR) processes the climate data, The International Research Institute (University of Columbia) provides analytical support and the generation of MapRooms, The European Space Agency (ESA) Earth Observation for Sustainable Development (EO4SD) initiative and the dedicated cluster on Climate Resilience accesses the earth-observation datasets ERA5 Land Product of European Commission's Copernicus Climate Change service in this portal. The data were downloaded via the portal based on the coordinates of the meteorological stations of the General Directorate of State Meteorology Affairs, located within the borders of Turkey. The distribution of 126 observation points determined in Turkey is shown in Fig. 1.

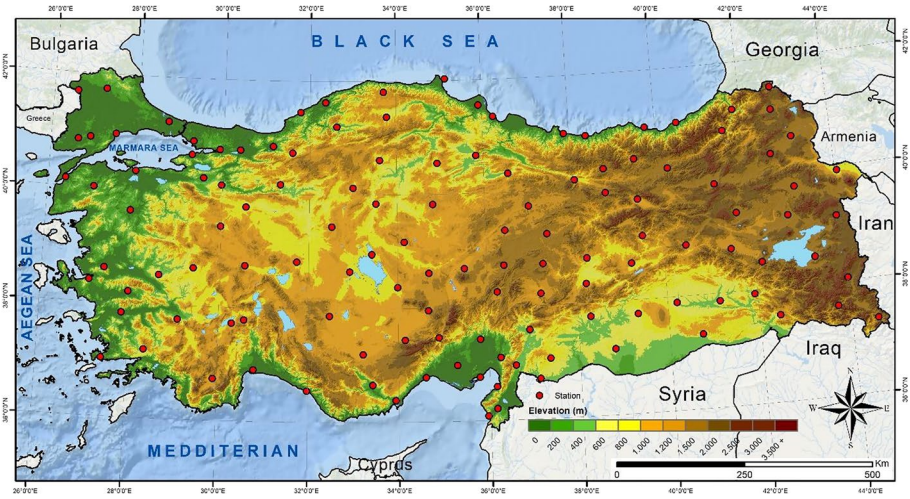


Fig. 1 The layout of the observational points in Turkey

2.2 Method

2.2.1 Standardized precipitation index (SPI) based on PE3 III distribution

The original SPI is traditionally calculated using the two-parameter Gamma distribution (Mckee et al. 1993). Blain and Meschiatti (2015) stated in their study that the standardized precipitation index detected drought in a normalized or standardized manner based on probability. However, its performance was affected by the two-parameter Gamma distribution used in its formulation, and this used distribution did not fully match the precipitation data. Therefore, drought analyses were performed with the Pearson Type III distribution. The SPI calculation stages based on PE3 start from Eq. 1 and continue to Eq. 7. The PE3 distribution's three parameters and its pdf can be defined as:

$$\mathrm{pe}(x) = \frac{(x-\xi)^{\alpha-1}\exp\left[\frac{(-x+\xi)}{\beta}\right]}{\beta^{\alpha}\Gamma(a)} \tag{1}$$

for $\gamma > 0$ and $\xi = \mu - 2\sigma/\gamma$, where μ, σ, γ are the location (mean value of the series), scale, and shape parameters, respectively. As Hosking and Wallis (1997) stated, there is no clear analytical form of the quantile function pe(x). Since Eq. 1 is undefined at $x < \mu - 2\sigma/\gamma$, the cumulative probability is:

$$\mathrm{Hp}(x) = qp + (1 - qp)\mathrm{PE}(x). \tag{2}$$

qp is the empirical probability of $x < \mu - 2\sigma/\gamma$ values, and

$$\mathrm{PE}(x) = \frac{G\left(\alpha, \frac{x-\xi}{\beta}\right)}{\Gamma(\alpha)}. \tag{3}$$

$G(.)$ is the incomplete gamma function. As Hosking and Wallis (1997) stated, if γ equals zero, the distribution is normal and the interval of x becomes $-\infty < x < \infty$. After the studies of Hosking and Wallis (1997) and Guttman (1999), parameter estimation is grounded on the methods of L-moments. Hosking (1990) asserted that L-moment fitting tends to be selected for small-sized data samples. The results of the two parameter estimation methods (L-moments and maximum probability) are generally similar for moderate- and large-sized samples. The SPI values for 3-month period were calculated based on PE3. It is important that the time scale associated with the SPI value is explained by the month at the end of the analysis period. For instance, the 3-month SPI value identified at the end of June is associated with the total precipitation observed in April, May, and June. Through PE3 probability distributions, the cumulative probability of the observed precipitation amount was calculated. Afterward, the inverse normal (Gaussian) function with mean zero and variance one is applied to the cumulative probability (Hp (x)), the result is SPI (Blain 2011).

$$\mathrm{SPI} = -\left(t - \frac{c_0 + c_1 t + c_2 t^2}{1 + d_1 t + d_2 t^2 + d_3 t^3}\right) \text{ for } \mathrm{Hp}(x) \le 0.5 \tag{4}$$

$$\mathrm{SPI} = +\left(t - \frac{c_0 + c_1 t + c_2 t^2}{1 + d_1 t + d_2 t^2 + d_3 t^3}\right) \text{ for } \mathrm{Hp}(x) < 1 \tag{5}$$

$$t = \sqrt{\ln\left(\frac{1}{H(x)^2}\right)} \text{ for } Hp(x) \leq 0.5 \tag{6}$$

$$t = \sqrt{\ln\left(\frac{1}{1 - H(x)^2}\right)} \text{ for } Hp(x) < 1 \tag{7}$$

$c_0 = 2.515517$; $c_1 = 0.802853$; $c_2 = 0.010328$; $d_1 = 1.432788$; $d_2 = 0.189269$; $d_3 = 0.001308$

This attempt focuses on calculating only the 3-month SPI, as 3-month SPI reflects short- and medium-term moisture conditions. It also supplies a seasonal estimation for precipitation. Several studies also revealed that a short-term (3-month) SPI provides an indication of the seasonal anomaly regarding precipitation, hence considered a meteorological drought indicator (Mckee et al. 1993; Hayes et al. 1999; Ji and Peters 2003; Foster et al. 2014; Kumar et al. 2014). SPI classification limits according to drought category are available in Table 1.

2.2.2 Drought characteristics

Time series of data values representing deficit or surplus of water compared to its average availability, in general, is made available through drought indices. Drought indices are also utilized in evaluating the drought characteristics. Drought indices use Theory of Runs (Yevjevich 1967) that demonstrate various attributes of drought in terms of intensity, duration, frequency, severity, and hazard. The Theory of Runs model is shown in Fig. 2. A threshold value is selected, which determines the beginning of a dry period. The dry period begins when the index value drops below the identified threshold values and continues until it becomes larger than the identified threshold value. The magnitude of droughts is calculated through this equation:

$$\text{DM} = -\left(\sum_{j=1}^{x} \text{SPI}_{3j}\right) \tag{8}$$

where j is the first month and $SPI_{3j}<$ threshold value and continues for x months till $SPI_{3j}>$ threshold value (Maccioni et al. 2015).

Table 1 SPI drought classification limits

Class	SPI, Standard value	Classification
1	> 2.00	Extremely wet (EW)
2	1.50–1.99	Very wet (VW)
3	1.00–1.49	Moderately wet (MW)
4	0.50–0.99	Slightly wet (SW)
5	0.00–0.50	Normal wet (NW)
6	0.00 to − 0.50	Normal dry (ND)
7	− 0.50 to − 0.99	Slightly dry (SD)
8	− 1.00 to − 1.50	Moderately dry (MD)
9	− 1.50 to − 2.00	Very dry (VD)
10	< − 2.00	Extremely dry (ED)

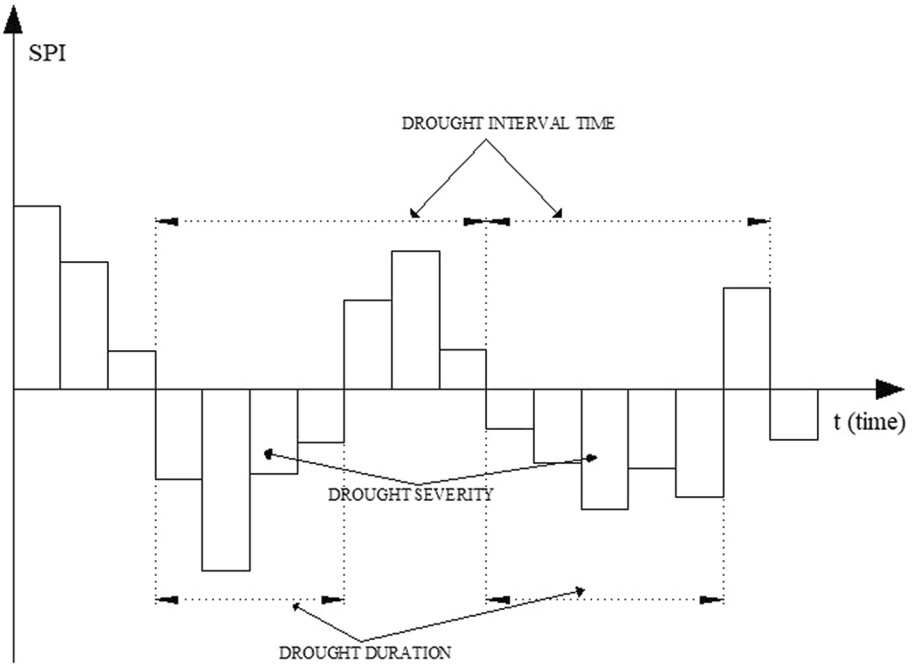


Fig. 2 The theory of runs model

The value "−1" was chosen as the threshold value *per* the representation of dry periods based on SPI values in Table 1 in this analysis. $-1 < \text{Value} < 0$ represents slightly dry conditions, whereas the value lesser than − 1 represents a moderate drought. Thus, under the moderate, very, and extreme conditions, value − 1 is chosen as the threshold value. The duration of drought is defined by the sum of consecutive months for which the index value lies below − 1 till it becomes greater than − 1. The index value should drop below the chosen threshold for at least 2 months to confirm that a dry event has occurred (Spinoni et al. 2014). Consequently, the minimum drought duration should last at least 2 months. Accordingly, the maximum drought duration for any district can be defined by the maximum number of consecutive months for which the dry event is defined. The measure of the average strength of the drought per month represents drought intensity. The intensity has been operationalized as the ratio of total magnitude to drought duration of a particular event for this study. The drought intensity was assessed on an event-basis for all districts to enable comparisons. If a greater scale of drought occurs over a minimal period, such as a few months, drought intensity is high, and its impact is severe. Dividing severity over duration provides the drought intensity for this study. Based on the value corresponding to the drought index, drought for a month can be classified as moderate, very, and extreme, as shown in Table 1. Drought frequency in percentage or percentage probability of occurrence of a drought of a particular category is calculated by the ratio of the number of dry months falling in that category and the total interval of the analysis (Singh et al. 2019).

$$\text{Probability } \% = \frac{\text{Total number of dry months}}{\text{Total number of months taken}} \times 100. \tag{9}$$

2.2.3 Mann–Kendall trend analysis

This study conducted a trend analysis to determine the increase or decrease in SPI values calculated by monthly total precipitation. SPI 3-month values were examined by Mann–Kendall trend analysis. The Mann–Kendall test is applied to test the alternative hypothesis ($H1$), the monotonic course of increasing or decreasing xi observations randomly ordered over time, against $H0$, i.e., null hypothesis. The data are assessed as sequential time series. Each data value is compared with the following data value. As a result of the comparisons, values are assigned to the sign function and the final value of the S statistic is obtained. The S statistic to be derived is the Mann–Kendall test statistic. In the present paper, The Mann–Kendall test is carried out with 5% level of significance. Detailed information can be found in reports provided by Salmi et al. (2002).

2.2.4 Joint return periods using copula functions

The copula functions were applied to generate multivariate distributions from univariate marginal distributions. Sklar (1959) formed the theoretical basis of this technique. Afterward, the definition of Archimedean copula functions, often used in the hydrological variable analysis, was defined by Genest et al. (2007). Copula functions are outlined as multivariate distribution functions, $P(x_1, \ldots, x_2)$, with uniformly distributed variables on the interval [0,1]:

$$P\left(x_1, \ldots, x_2\right) = C\left[P\left(x_1\right), \ldots, P(x_{n)}\right] = C\left(u_1, \ldots, u_n\right) \tag{10}$$

where $P(x_i)$ is the marginal distribution of x_i, uniform on the interval l [0,1], also is denoted by u_i the $P(\ldots)$ in the left-hand side is the joint probability distribution and C is the Cumulative Distribution Function (CDF) of the copula. These work-tested copula functions of three families are frequently used in drought analyses among several existing Archimedean copula families. It is possible to estimate the parameter θ of the copula functions by the relationships shown in the third column of Table 2, given that the series of S (severity) and D (duration) have a correlation (linear or nonlinear) to each other expressed by the Kendall correlation (τ). The copula was compatible for modeling the properties of the drought in order to select the Akaike information criterion (AIC) (Eq. 11) for whole period (1925–2016):

$$\mathrm{AIC} = 2k - 2\ln\left(\hat{L}\right) \tag{11}$$

Table 2 Archimedean copulas: families of tested functions

Family	Bivariate copula	Relationship between τ and θ
Gumbel–Hougaard	$exp = \left\{-\left[(-lnu_1)^{\theta} + (-lnu_2)^{\theta}\right]^{\frac{1}{\theta}}\right\}$	$\tau = 1 - \frac{1}{\theta}$
Clayton	$max\left(\left[{u_1}^{-\theta} + {u_2}^{-\theta} - 1\right]^{\frac{-1}{\theta}}, 0\right)$	$\tau = \frac{\theta}{\theta+2}$
Frank	$-\frac{1}{\theta} ln\left[1 + \frac{(e^{-\theta u_1}-1)(e^{-\theta u_2}-1)}{(e^{-\theta}-1)}\right]$	$\tau = 1 + \frac{4}{\theta}\left[\frac{1}{\theta}\int_0^{\theta} \frac{t}{e^t-1} dt - 1\right]$

where the model $\widehat{L}$ is the maximum value of the likelihood and k is the number of the estimated parameter. The most suitable copula for the observation point is identified by the copula function that has the lowest AIC value. In this study, Bayesian information criterion (BIC) (Eq. 12) was also used to identify the best-performing copula function. The lower BIC value signals a better copula function.

$$BIC = k(\ln(n)) - 2\ln\left(\hat{L}\right). \tag{12}$$

In Eq. 12, n is the number of observations.

Frequency analysis or the recurrence interval or return period of hydrologic events is used as a typical method in hydraulic and hydrologic design (Shiau and Shen 2001). The estimation of drought return periods can be considered as valuable information, especially, for a proper water use under drought conditions (Serinaldi et al. 2009). The average elapsed time or mean interval time between occurrences of and bivariate drought events defines the return period of a drought (Chen et al. 2011).

The return period can be defined as the average time passed or average inter-arrival time between critical cases. Drought is bi-variable event and is represented by the duration (D) and severity (S) of drought. Thus, the joint and conditional characteristics of the period play a major role in the calculations for determining the frequency of drought. The return period formulated for drought risk has two major factors, drought events [$D \geq d$ and $S \geq s$] and drought events with [$D \geq d$ or $S \geq s$]. The copula-based joint return period of drought can be formulated along these lines (Katipoğlu and Can 2018).

$$T_{\text{and}} = \frac{E(L)}{P(D \geq d \text{and} S \geq s)} = \frac{E(L)}{1 - F_D(d) - F_S(s) + F_{DS}(d,s)} = \frac{E(L)}{1 - F_D(d) - F_S(s) + C\left(F_D(d), F_S(s)\right)} \tag{13}$$

$$T_{\text{or}} = \frac{E(L)}{P(\text{D} \geq \text{d or S} \geq \text{s})} = \frac{E(L)}{1 - F_{\text{DS}}(d,s)} = \frac{E(L)}{1 - C\left(F_D(d), F_S(s)\right)} \tag{14}$$

where T_{and} refers to the joint return period for the probability of surpassing both of drought duration and severity ($D \geq d$ and $S \geq s$), T_{or} refers to the joint return period for the probability of surpassing either one of the drought duration and severity ($D \geq d$ or $S \geq s$), and E(L) is the expected drought inter-arrival time. The time between consecutive arrivals defines the inter-arrival time (Katipoğlu and Can 2018).

The return periods were obtained through the copula functions calculated as ($S = 3$, $D = 3$) for weak drought, ($S = 6$, $D = 6$) moderate drought, and severe drought ($S = 9$, $D = 9$) using the criteria in Wang et al. (2018) study. Through this, the empirical return period of the average droughts of each season and the return period of the most severe drought ever recorded in the time span covered by the precipitation series could have been obtained (Júnior et al. 2020). Unlike Theory of Runs, the drought threshold was determined as "0" in calculating S and D, because Theory of Runs usually takes the drought threshold as "− 1" for seasonal drought severity and duration. Since S and D values for copula functions are calculated for overall, not seasonal, the drought threshold was taken as "0." This study also examined how drought severity changes in various return periods. The spread of drought severity has been investigated in Turkey in 2-, 5-, 10-, 20-, 50-, and 100-year return periods.

2.2.5 Visualization using GIS

The Inverse Distance Weighting Method (IDW) was adopted to monitor the areal distribution of drought visually in study area. IDW is a simple interpolation model to predict the unknown sample point values through the weighted average of nearby known sample point values. The IDW calculator Z_p is determined as in Eq. 15.

$$Z_p = \frac{\sum_{i=1}^{n} \frac{Z_i}{d_i^p}}{\sum_{i=1}^{n} \frac{1}{d_i^p}}. \tag{15}$$

The Z_p is the estimated value of variable z at point i, Z_i is the sample value at point i, d_i is the distance of the sample point to the estimated point, n is the number of total sample points, p is the power that determines the weight based on the distance. A software known as ArcGis was used for mapping in this regard.

3 Results

3.1 Seasonal SPI results for the case of Turkey

The first part of the study presented seasonal SPI values recorded between 1925 and 2016. Monthly total precipitation data are arranged separately for spring, summer, autumn, and winter. Since the seasonal analysis is used in this study, the 3-month SPI calculation, which analyzes seasonal drought, in particular, is emphasized. In this study, the seasonal precipitation amount in any year was obtained by dividing the monthly total precipitation amount by the number of months in the season. For instance, rainfall in the autumn season of 1988 was calculated by the arithmetic average of the monthly total precipitation amounts of September, October, and November. Three-month SPI values obtained according to the monthly total rainfall data for 1925–2016 are shown in Fig. 3.The left column of Fig. 3 shows the seasonal precipitation values varying by years for the whole of Turkey.

Accordingly, the most precipitation falls in the spring season in Turkey. Spring is followed by the winter and autumn seasons, respectively. The least precipitation falls in the summer season. The average seasonal precipitation in Turkey is 59.02 mm in spring, 21.62 mm in summer, 43.48 mm in autumn, and 49.51 mm in winter. The overall seasonal average minimum rainfall in Turkey was 32.85 mm in spring 1947, 11.06 mm in summer 1928, 14.26 mm in autumn 1926, and 36.01 mm in winter 1932. The highest seasonal average rainfall recorded was 87.18 mm in spring 1963, 39.25 mm in summer 1972, 72.59 mm in the autumn 1942, and 61.89 mm in the winter in 1940. Seasonal SPI values corresponding to seasonal precipitation amounts are shown in the right column of Fig. 3.

Accordingly, the lowest and highest SPI values in the spring were − 2.12 (extreme dry) in 1972 and 1.77 (very wet) in 1963, the lowest and highest SPI values of summer were − 1.50 (moderate dry) in 2003 and 0.72 (slightly wet) in 1939, the lowest and highest SPI values in autumn were − 1.77 (very dry) in 1928 and 0.84 (slightly wet) in 1996, the lowest and highest SPI values in winter were − 1.99 (very dry) in 1930 and 2.14

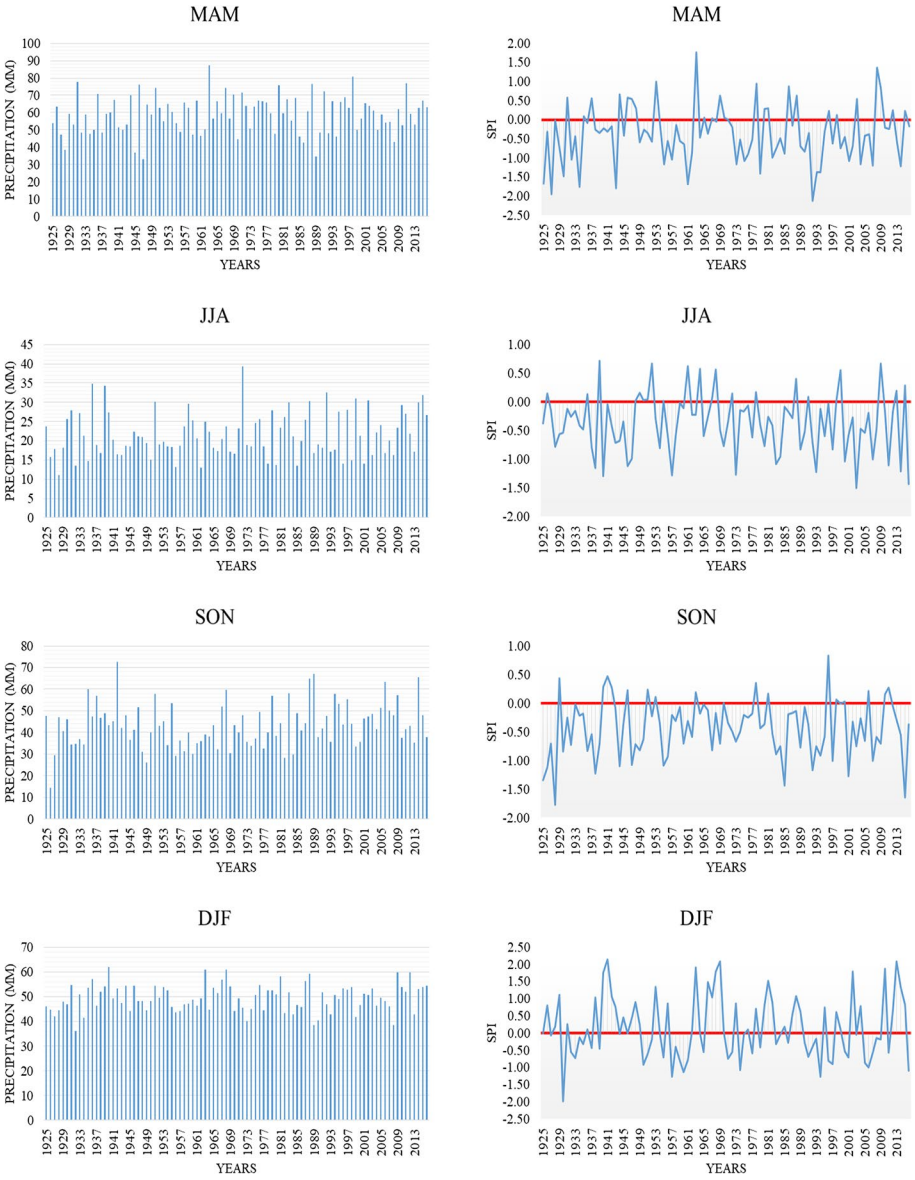


Fig. 3 Rainfall (left) and SPI graphs (right) for all 4 seasons in Turkey

(extreme wet) in 1941, were recorded, respectively. These results revealed that the lowest SPI value was recorded in spring and the highest SPI value in winter. Besides, the seasonal SPI graphs in Fig. 3 indicate that the autumn season was the driest in general.

Periodic drought frequency results obtained with Eq. 9 are available in Table 3. The most normal dry conditions were experienced in the spring and summer months in the 1925–1949 period with a rate of 40%. The incidence of 16% very dry conditions in the spring season is striking regarding this period. Normal dry conditions were observed with

Table 3 Drought frequency values for 4 different periods and 4 different seasons according to the drought category across Turkey

	Drought frequency (%)							
	MAM	JJA	SON	DJF	MAM	JJA	SON	DJF
	1925–1949				1950–1974			
EW	0.0	0.0	0.0	4.0	0.0	0.0	0.0	4.0
VW	0.0	0.0	0.0	4.0	4.0	0.0	0.0	8.0
MW	0.0	0.0	0.0	12.0	4.0	0.0	0.0	12.0
SW	20.0	4.0	0.0	12.0	4.0	16.0	0.0	8.0
NW	8.0	16.0	20.0	24.0	16.0	20.0	16.0	12.0
ND	40.0	40.0	24.0	32.0	32.0	36.0	52.0	12.0
SD	8.0	28.0	32.0	8.0	24.0	20.0	28.0	32.0
MD	8.0	12.0	20.0	0.0	12.0	8.0	4.0	12.0
VD	16.0	0.0	4.0	4.0	4.0	0.0	0.0	0.0
ED	0.0	0.0	0.0	0.0	0.0	0.0	0.0	0.0
	1975–1999				2000–2016			
EW	0.0	0.0	0.0	0.0	0.00	0.00	0.00	5.88
VW	0.0	0.0	0.0	4.0	0.00	0.00	0.00	11.76
MW	0.0	0.0	0.0	4.0	5.88	0.00	0.00	5.88
SW	12.0	4.0	4.0	28.0	11.76	5.88	0.00	17.65
NW	16.0	16.0	12.0	12.0	11.76	11.76	23.53	0.00
ND	16.0	40.0	44.0	32.0	35.29	35.29	29.41	17.65
SD	36.0	32.0	28.0	16.0	11.76	11.76	29.41	35.29
MD	16.0	8.0	12.0	4.0	23.53	29.41	11.76	5.88
VD	0.0	0.0	0.0	0.0	0.00	5.88	5.88	0.00
ED	0.0	0.0	0.0	0.0	0.00	0.00	0.00	0.00

a frequency of 52% in the autumn season in the 1950–1974 period. Similarly, 44% frequency normal dry conditions were recorded in the autumn season for the 1975–1999 period. Finally, normal dry conditions were reported with a maximum rate of 35.29% in spring and summer for the 2000–2016 period. Table 3, in general, illustrates that the frequency of moderate dry has increased from 1925 to 2016. The results showed that normal dry conditions were recorded mostly according to the rate of drought seasonally throughout Turkey. Moreover, Turkey is a normal dry country in general. The wet conditions indicate that the rate of extreme wet was the highest in the 2000–2016 period. The lowest rates were recorded during the 1925–1949 and 1950–1974 periods. The highest slightly wet frequency was 20% in the spring season of 1925–1949.

The second stage of the study covers the years 1925–2016, in which monthly total precipitation data are available and divided into 25-year periods. It was aimed to monitor the evolution of drought situation for every 25 years. Table 4 presents the drought categories on an annual basis. It is understood from the table that the spring season of 1926, 1928, 1935, 1944, autumn season of 1929, and the winter season of 1931 were recorded as very dry between the years 1925–1949. There were no very or extreme dry conditions in the summer during this period. The winter of 1942 was extremely wet. Extreme wet conditions

Table 4 Drought categories of the seasons by years across Turkey

TURKEY																
1925-1949					1950-1974				1975-1999				2000-2016			
	MAM	JJA	SON	DJF	MAM	JJA	SON	DJF	MAM	JJA	SON	DJF	MAM	JJA	SON	DJF
1	VD	ND	MD	-	ND	NW	SD	SD	MD	ND	ND	ND	ND	MD	NW	SD
2	ND	NW	MD	SW	ND	NW	NW	SD	SD	ND	ND	NW	MD	SD	MD	SD
3	VD	ND	SD	ND	SD	SW	ND	ND	SD	SD	ND	SD	SD	ND	ND	VW
4	ND	SD	VD	NW	MW	ND	NW	MW	SW	ND	NW	SW	SW	VD	SD	ND
5	SD	SD	NW	MW	ND	SD	ND	ND	MD	ND	ND	ND	MD	ND	ND	SW
6	MD	SD	SD	VD	MW	NW	MD	SD	NW	SD	ND	SW	ND	SD	SD	SD
7	SW	ND	ND	NW	SD	SD	SD	SW	NW	ND	NW	VW	ND	ND	NW	SD
8	MD	ND	SD	SD	MD	MD	ND	MD	SD	ND	SD	SW	MD	MD	MD	SD
9	ND	ND	ND	SD	ND	SD	ND	ND	SD	MD	SD	ND	MW	ND	SD	ND
10	VD	ND	ND	ND	SD	ND	ND	SD	ND	SD	SD	ND	SW	SW	SD	ND
11	NW	ND	ND	ND	SD	ND	SD	MD	SD	ND	MD	NW	ND	ND	NW	VW
12	ND	NW	SD	NW	VW	SW	ND	SD	SW	ND	ND	ND	ND	MD	NW	SD
13	SW	SD	SD	ND	SD	ND	SD	NW	ND	ND	ND	SW	NW	ND	ND	SW
14	ND	MD	MD	MW	VW	ND	NW	VW	SW	NW	ND	MW	SD	NW	ND	EW
15	ND	SW	SD	ND	ND	SW	ND	NW	SD	SD	SD	SW	MD	MD	SD	MW
16	ND	MD	NW	VW	NW	SD	ND	SD	SD	SD	ND	ND	NW	NW	VD	SW
17	ND	ND	NW	EW	ND	ND	ND	MW	ND	NW	ND	SD	ND	MD	ND	MD
18	ND	ND	NW	MW	NW	NW	SD	MW	ED	SD	MD	ND				
19	VD	SD	ND	SW	ND	SW	ND	VW	MD	MD	SD	ND				
20	SW	SD	MD	ND	SW	ND	ND	EW	MD	ND	SD	MD				
21	ND	ND	ND	NW	NW	SD	NW	NW	ND	SD	SD	SW				
22	SW	MD	NW	ND	NW	ND	ND	SD	NW	ND	SW	SD				
23	SW	SD	MD	NW	ND	NW	ND	SD	SD	SD	MD	SD				
24	NW	NW	SD	SW	MD	MD	SD	SW	NW	NW	NW	SW				
25	SD	NW	SD	NW	SD	ND	ND	MD	SD	SW	NW	NW				

were not recorded in the 1950–1974 period while they were documented in the winter of 1969. Extreme dry conditions were observed in spring 1992, while there were no extreme wet conditions in the 1975–1999 period. Very dry conditions were documented in summer 2003 and autumn 2015 in the period of 2000–2016. Moreover, extreme wet conditions were reported in winter 2013. These results show that the driest period was the 1925–1949 period.

Periodic and seasonal drought maps obtained with IDW are shown in Figs. 4, 5, 6, and 7. These maps facilitate the interpretation of wet and dry conditions in Turkey for spatial and temporal contexts. Figure 4 reveals a striking finding regarding normal dry conditions observed throughout Turkey. For the spring season, the 1925–1949 period is observed to be normally wet in the eastern part of the country (excluding the Northeast), the inland parts of the Southeast and the Eastern Mediterranean region and the western Aegean coasts. There are also observational spots that are slightly wet in the east of the country. During the 1950–1974 period, the area of normal wet conditions narrowed in the eastern region, as the Western Black Sea and its inner parts are determined as normal wet. In the Central Anatolian part of the country (around Tuz Gölü/Salt Lake) and in the southeastern

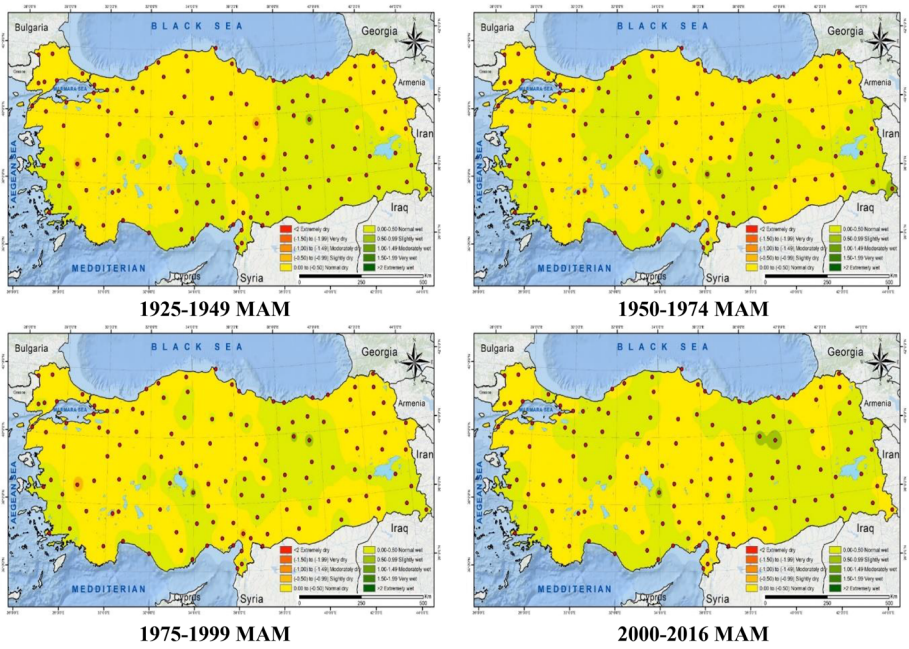


Fig. 4 Spring season drought maps for 4 different year periods

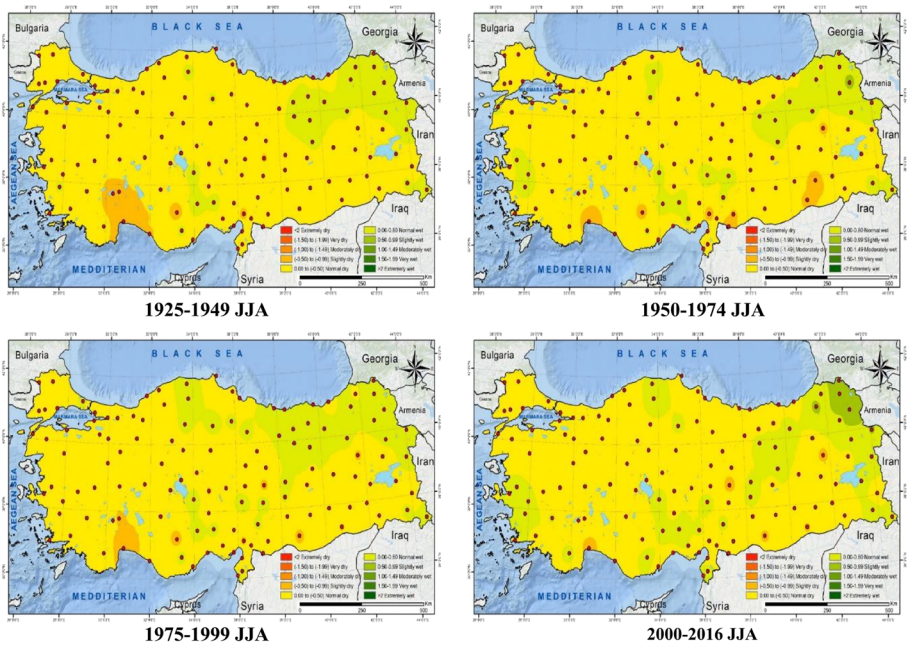


Fig. 5 Summer season drought maps for 4 different year periods

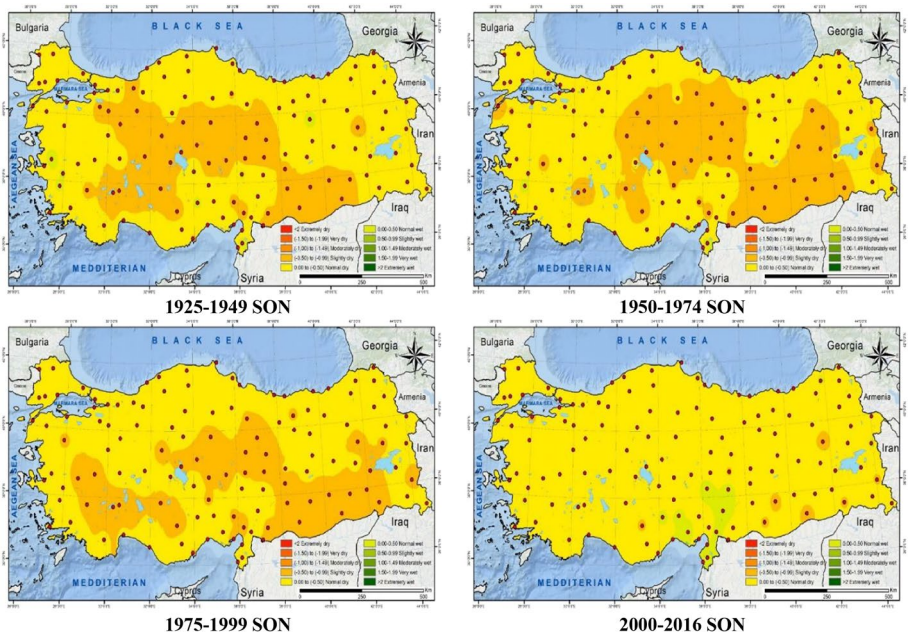


Fig. 6 Autumn season drought maps for 4 different year periods

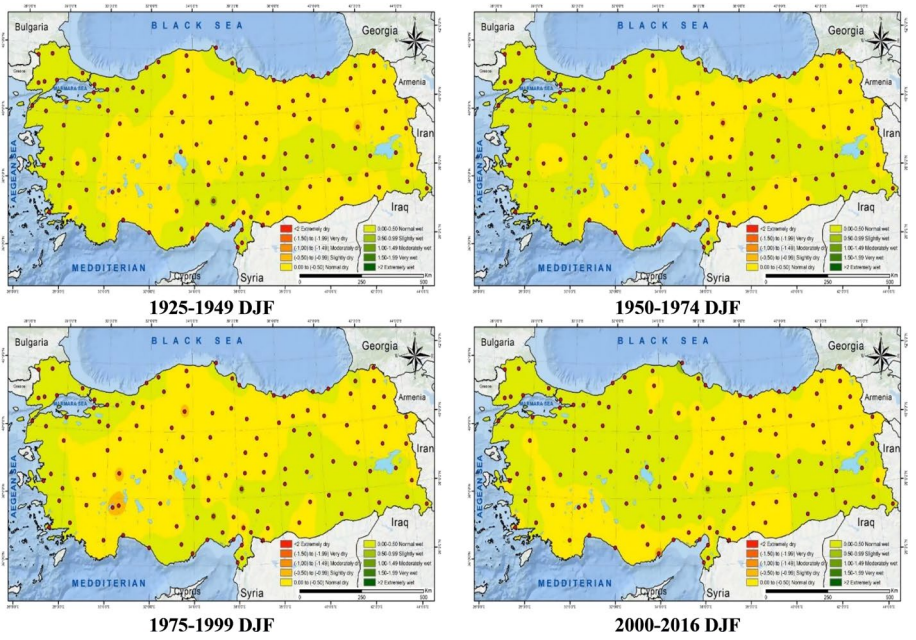


Fig. 7 Winter season drought maps for 4 different year periods

end of the Eastern Anatolia Region, slightly wet situations were recorded. The 1975–1999 period is similar to 1925–1949 in terms of spatial distribution. However, slightly dry conditions have been determined in the inner Aegean. Slightly wet situations continued in the west of the Eastern Anatolia Region. The 2000–2016 period has a very similar profile with the 1950–1974 period. Only the spatial spread of slightly wet cases in the west of Eastern Anatolia has increased.

Besides, Fig. 5 illustrates that the western Mediterranean coasts and inner parts were slightly dry while the eastern part and the northeast of the country were normally wet in the summer seasons during 1925–1949. The area in the Western Mediterranean narrowed slightly in the 1950–1974 period, as slightly dry situations emerged in the Southeast regions. Local slightly wet conditions were reported in the northeastern region. Similar patterns continue in the 1975–1999 period by increasing the normal wet spatial distribution in the inner parts of the Central Black Sea Region. Slightly wet conditions were reported in the 2000–2016 period, especially in the northeastern regions of the country expanded these areas.

Figure 6 shows that a large part of Central Anatolia, the whole of the Southeastern Anatolia Region, and the inner parts of the Western Mediterranean Region are slightly dry in the autumn seasons of the 1925–1949 period. Slightly dry conditions widened their area in the 1950–1974 period, especially in Eastern Anatolia and Southeastern Anatolia Regions. Slightly dry situations widened their zone in the 1975–1999 period in the east of the Inner Aegean and Eastern Mediterranean Regions. Moreover, slightly dry conditions were recorded very rarely in the 2000–2016 period, while normal wet conditions were detected in the Eastern Mediterranean Region.

Figure 7 reveals that in the winter seasons of the 1925–1949 period, almost all of Turkey's Marmara, Western Black Sea, Aegean (normal wet conditions continue locally in the Inner Aegean), the Eastern Mediterranean, and the south of Eastern Anatolia display predominantly wet conditions. The 1950–1974 period draws a similar profile. It was understood that the Marmara, Coastal Aegean, Central and Eastern Mediterranean, Southeastern Anatolia (local normal wet conditions continue), and the south of Eastern Anatolia were normally wet in the 1975–1999 period. Moreover, slightly dry conditions were recorded locally in the inner parts of the Western Mediterranean Region. It can also be stated that the entire region of Marmara and Central Anatolia (normal dry conditions continue in the east), the coastal Aegean and the western parts of the Southeastern Anatolia, and the inner parts of the Eastern Mediterranean were normally wet in the 2000–2016 period.

3.2 Mann–Kendall trend results of Turkey

Figure 8 illustrates the spatial distribution of Mann–Kendall trend analysis results in Turkey for the 1925–2016 period covering the entire time period. Test Z significance values are coded among themselves and recorded on the map. The spring season shows a statistically insignificant decrease throughout Turkey. This means that drought tends to increase. However, a statistically nonsignificant increase has been detected in the inner parts of the Western Mediterranean, West Marmara and the East of North East Anatolia, and the north and east of Central Anatolia which means drought tends to decrease. However, the 1925–2016 spring map revealed a statistically significant decrease in the West Mediterranean coasts, west of West Marmara, the east of Central Anatolia, and the inner parts of the Central Black Sea Region, and the Northeastern Anatolia Region locally. Thus, drought has been increasing in these areas.

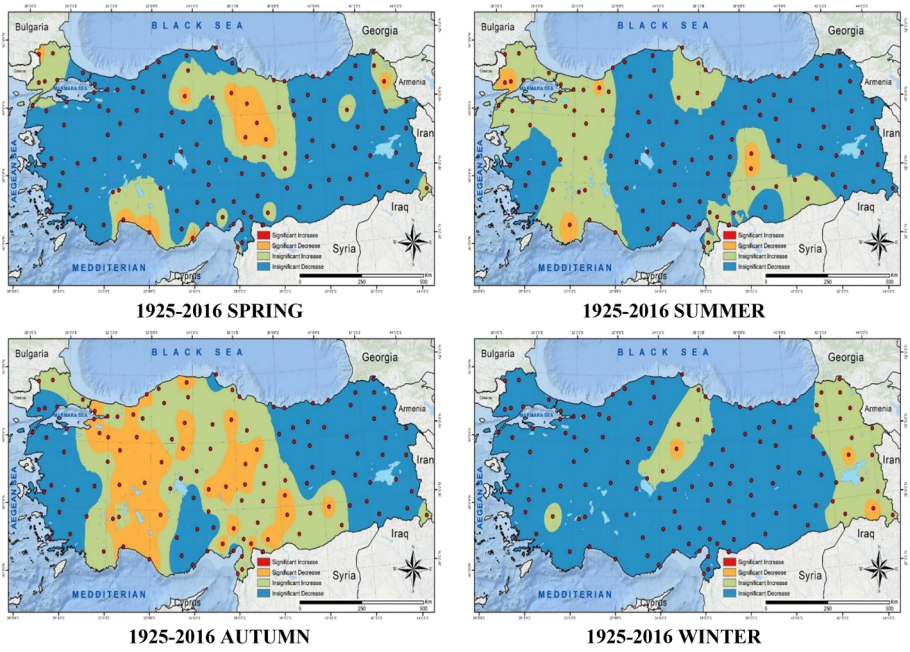


Fig. 8 Mann–Kendall trend maps for the 4 season during 1925–2016

The insignificant decrease continues in the eastern and central parts of the country in the summer seasons. An insignificant increase was observed in the Middle Black Sea Region, Western Mediterranean, Marmara and North Aegean, and parts of the eastern Mediterranean. A significant decrease draws attention in the south of West Marmara, the west of the Western Mediterranean, and the North of Southeastern Anatolia locally.

Moreover, a significant decrease has expanded its spatial distribution in the autumn season. Significant decreases have been detected in all of the west of Central Anatolia, a part of the east, a large part of the Western Mediterranean, parts of the Eastern Mediterranean, and Southeastern Anatolia. Some insignificant decreases have been detected in all parts of the Inner Aegean, Eastern Anatolia, Eastern Black Sea, and Eastern Mediterranean. Significant decrease is most evident in autumn seasons.

The insignificant decrease trend in the winter season is dominant in almost all of Turkey except the eastern part of Eastern Anatolia. Insignificant increase is dominant only in the east of Inner Anatolia, the east of Eastern Anatolia, and the inner parts of the Southern Aegean. A significant decrease trend has been observed locally in these regions. If we interpret the Mann–Kendall trend maps in general, there is an increase in drought at an insignificant level throughout Turkey. There was a significant increase in drought especially in the autumn seasons.

3.3 Drought characteristics using Theory of Runs results of Turkey

Figure 9 contains drought intensity maps calculated using drought severity and drought duration obtained with Theory of Runs model. The drought intensity for an observational point is calculated by dividing the drought severity of that point by the drought duration of

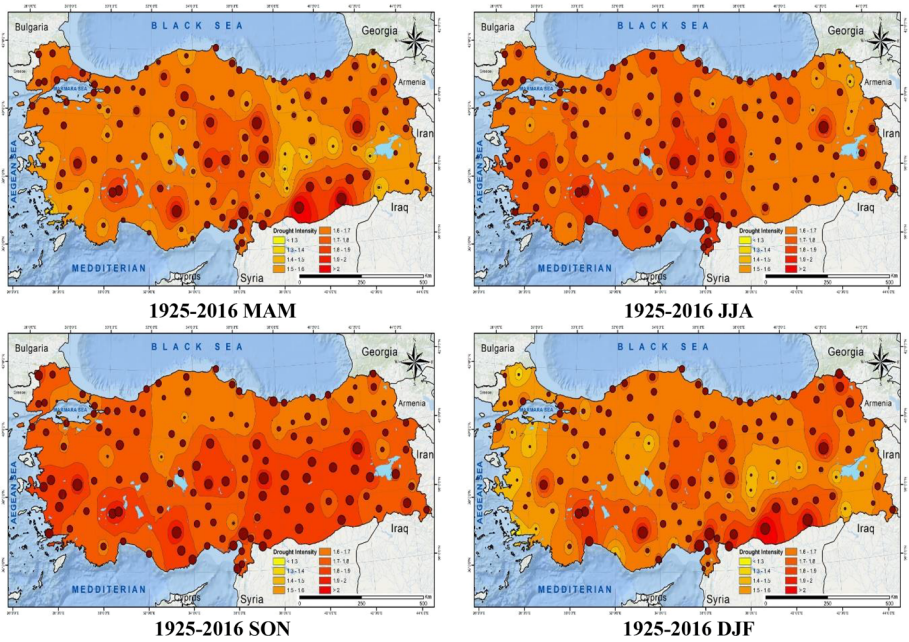


Fig. 9 Drought intensity maps for the 4 season during 1925–2016

that point. Turkey's overall drought intensity values obtained through 126 observational points were 1.662, 1.705, 1.760, 1.663 for spring, summer, autumn, and winter seasons, respectively. The maps in Fig. 9 reveal that the drought intensity is the highest (intensity is above "2") especially in southeastern Turkey during spring. Density is observed in the inner parts of the western Mediterranean, the south and east of Central Anatolia, and the east of the Eastern Mediterranean. It is the least in the west of Eastern Anatolia and on the Aegean coasts. It was observed that drought was intense in the Mediterranean Region, Coastal Aegean, and Central Anatolia during summers. The least intensity in summer was in the northeastern parts of Turkey. It can also be stated that drought intensity has increased in autumns throughout Turkey. It was also found that drought intensity values are high in a wide area, especially in the southeastern parts of Turkey. Another finding was that the drought is particularly intense in Southeastern Anatolia in winter seasons. Drought intensity values were above "2." The drought intensity is lowest in Marmara, Coastal Aegean, Central parts of Central Anatolia, and west of Eastern Anatolia. Drought intensity values were between 1.6 and 1.8 in the northeastern regions.

3.4 Drought return periods results of Turkey using copula functions

Frequency analysis regarding the drought characteristics is a key method in assessing the adequacies of water supply systems under dry conditions. A number of attempts have focused on univariate frequency analysis of the droughts, however they did not seek for the dependence between drought characteristics, such as duration and severity. Design and management of water supply systems necessitate to know joint (or conditional) probability properties besides the drought duration or severity only. Thus, bivariate frequency analyses

on drought events have become more popular in recent years. This study presents an example with copula functions for bivariate frequency analysis of the meteorological drought events in Turkey. Figure 10 shows the results of the joint return period. S and D values were calculated by taking the drought threshold as "0." The joint return period results were found by means of Eqs. 13 and 14. AIC and BIC were found to be − 303.37, − 309.99, and − 315.16; − 381.11, − 387.35, − 394.69, respectively, for Gumbel–Hougaard, Clayton, and Frank, respectively. According to AIC and BIC results, it was determined that the best copula function in Turkey is the Frank copula function. A certain exceedance probability associates usually with the return period of drought occurrence. A specific drought event may occur more than once in one single year and may also last for several months, which is not likely with a flood frequency analysis. At that point, for estimating return periods of drought events, drought characteristic, expected drought interval time is essential. Frank copula function, chosen as the most suitable fit, has been employed to calculate the joint return period of drought severity and duration in this research. Joint return period values

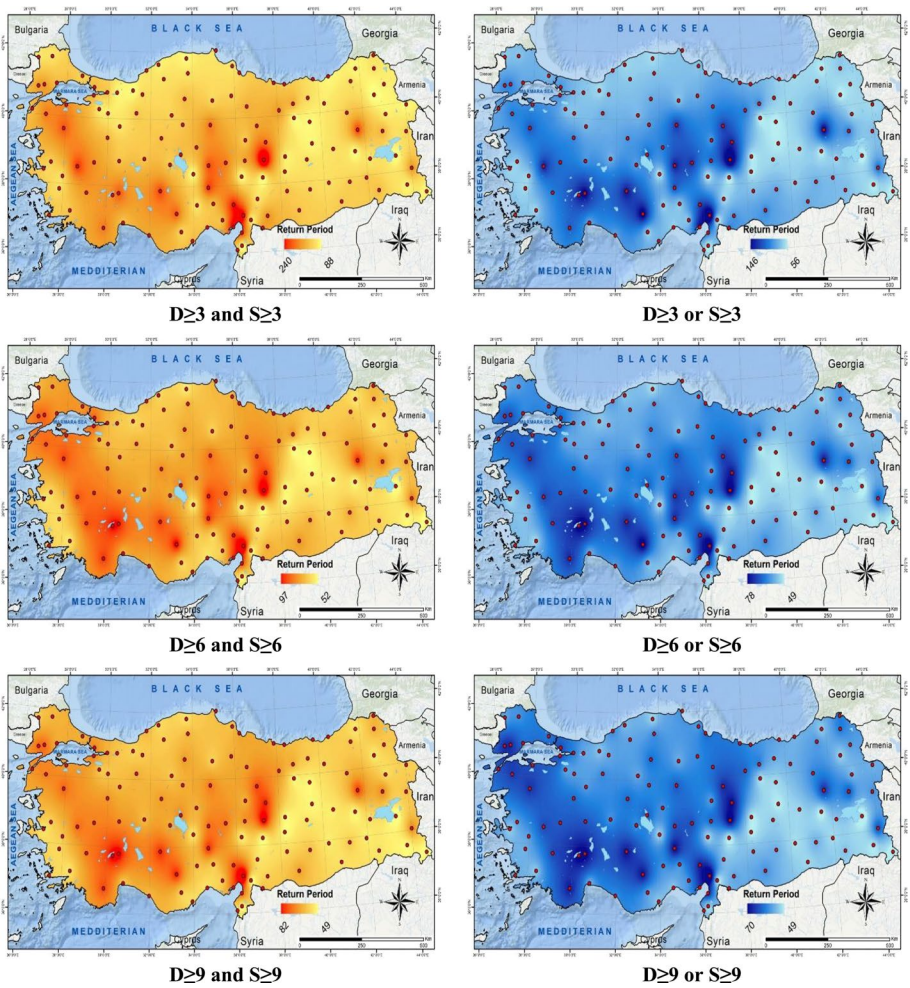


Fig. 10 Return period (months) for weak drought, moderate drought, and severe drought

were found for 3 different drought types: Weak drought ($S=D=3$), moderate drought ($S=D=6$), and severe drought ($S=D=9$). The ($D\geq d$ and $S\geq s$) and ($D\geq d$ or $S\geq s$) conditions were examined for 3 different drought types and the results obtained were mapped.

Considering the results of ($D\geq 3$ and $S\geq 3$) and ($D\geq 3$ or $S\geq 3$) for Turkey in general, the return period of weak drought for Turkey in general is 127.53 and 78.96 months, respectively. The return period ($D\geq 3$ and $S\geq 3$) ranges from 88 to 240 months ($D\geq 3$ or $S\geq 3$), from 56 to 146 months. In the case of ($D\geq 3$ and $S\geq 3$), the place where the return period is the highest for Turkey in general is the east of the Eastern Mediterranean Region and the western end of the Eastern Anatolia Region. In the case of ($D\geq 3$ or $S\geq 3$), the places where the maximum return period is recorded, besides the previous one, are seen locally in the inner parts of the western Mediterranean and the south of the Central Anatolia Region and the Eastern Anatolia Region. In both joint cases, the lowest return period values are observed in the Aegean coasts, the west of the Eastern Mediterranean, and the Southeastern Anatolia Region.

The return period of the moderate drought for the case ($D\geq 6$ and $S\geq 6$) and ($D\geq 6$ or S) 6) is 68.85 and 59.60 months, respectively. While the return period ($D\geq 6$ and $S\geq 6$) ranges from 52 to 97 months, ($D\geq 6$ or $S\geq 6$) ranges from 49 to 78 months.

For the case of ($D\geq 9$ and $S\geq 9$) and ($D\ S\ 9$ or $S\geq 9$), the return period of severe drought is 60.28 and 57.65 months, respectively. While the rotation period ($D\geq 9$ and $S\geq 9$) varies between 49 and 82 months, the rotation period ($D\geq 9$ or $S\geq 9$) varies between 49 and 79 months. The spatial spread of moderate and severe drought across Turkey is similar to weak drought. However, if we look at the results in general, while the return period of the weak drought is the highest, the return period of the severe drought is the lowest. In other words, severe drought is more common throughout Turkey. In this study, the return period results made with "and" appears higher than the return period results made with "or."

Finally, drought severity values were obtained for the ($D\geq 6$ and $S\geq 6$) model according to the return periods of 2, 5, 10, 20, 50, and 100 years. In the maps in Fig. 11, Turkey-wide results can be seen. According to the results, it is predicted that especially in the 100-year period, the drought severity values of the Central Anatolia Region will be high. In the south of Central Anatolia, drought severity has been higher in every period. On the other hand, the inner parts of the western Mediterranean have high drought severity values, except for a period of 50 years. In the east of the Eastern Mediterranean, drought severity values are high, except for periods of 50 and 100 years. Periods of 50 and 100 years are important for water resources planning.

4 Discussion

Drought risk is still a major concern in Turkey regarding the regions where precipitation totals are low and extremely variable. The combination of precipitation shortage and other climatic factors, such as high temperature, creates a substantial drought risk in the central and southeastern parts of Turkey, where agriculture is the main economic locomotive. The sudden decrease in subtropical belt precipitation, which started in the 1960s, started to influence the Eastern Mediterranean Basin and Turkey during the 1970s. Significant reduction trends in precipitation and drought events emerged more prominently in the winter season (Kapluhan 2013). The Aegean, Mediterranean, Marmara, and Southeastern Anatolia regions were most affected by the dry conditions between the early 1970 and 1990s. The most severe and widespread drought events occurred in 1973, 1977, 1990, and 1991. A

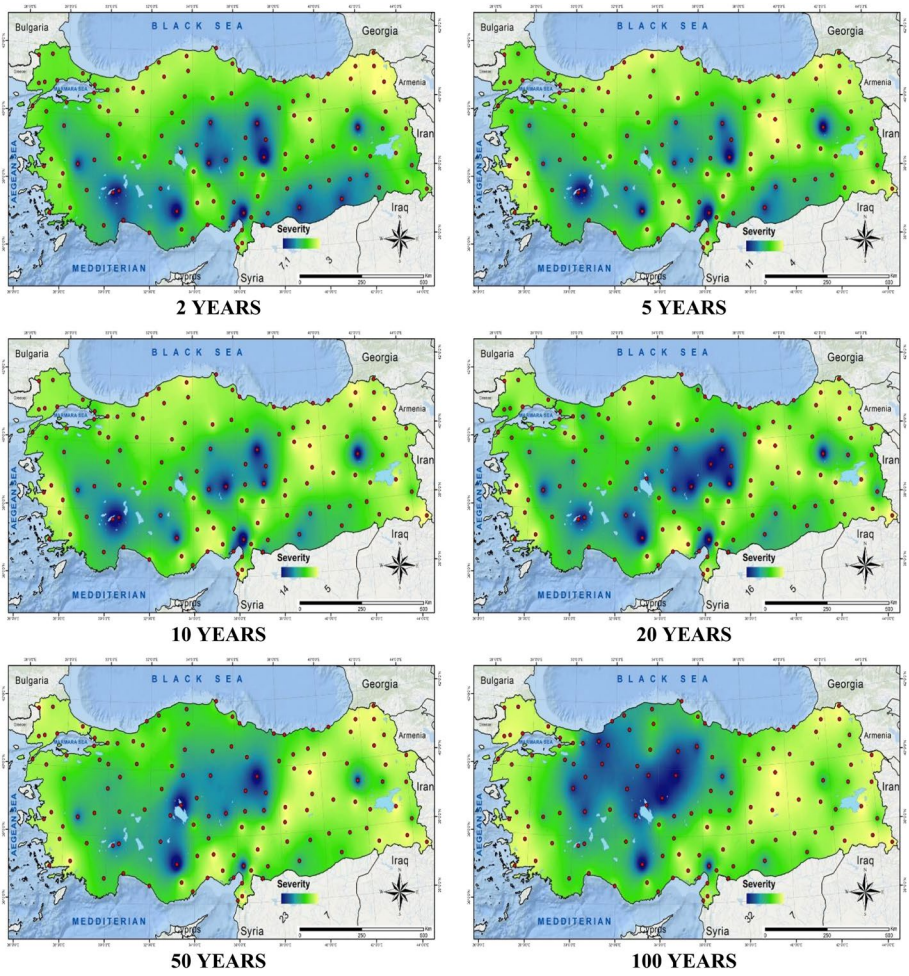


Fig. 11 Spatial variation of drought severity with different return periods of 2, 5, 10, 20, 50, and 100 years ($D \geq 6$ and $S \geq 6$)

significant decrease in precipitation or meteorological droughts were not observed in most of Turkey in the 1994–1998 period, except for the Eastern Anatolia Region. Afterward, drought events were recorded again in a large portion of Turkey in the years 1999–2000 and the first 3 months of 2001. Severe and widespread meteorological droughts were especially impactful in Eastern and Southeastern Anatolia and Aegean and Mediterranean regions. Agricultural and hydrological droughts have also occurred in Turkey as a result of meteorological droughts due to precipitation conditions far below the long-term averages. Water shortage and issues have reached a critical point not only in terms of agriculture and energy production, but also water resources management, which includes irrigation, drinking water, other hydrological systems, and activities. The significant decreasing trends observed in the annual and especially winter precipitations of the Eastern Mediterranean Basin and overall may be related to the decrease observed in the frequency of frontal midlatitude and Mediterranean low pressures prevailing in this region, especially in winter, and

the increases observed in high pressure conditions. Moreover, a weak upward trend was observed in the spring and summer precipitations of some stations with terrestrial precipitation regimes. The meteorological conditions that have led to the dominance of dry conditions in Turkey in the last 30 years can be explained mostly with the changes in circulation systems and the North Atlantic Oscillation. Weakening of the Siberian Anticyclone after 1980 (winter drought), the Azores anticyclone ridge reaching the Eastern Mediterranean (winter drought), the scarcity of frontal systems coming to the Mediterranean, the northward insertion of the Basra low pressure (summer droughts) and the consolidation of the Azores and Basra low pressures (summer droughts). Furthermore, the positive cycles of the North Atlantic Oscillation (NAO) are quite compatible with the dry conditions in Turkey (Kapluhan 2013).

Türkeş (1996) frames some spatial and temporal characteristics of Turkey's precipitation, mainly in terms of drought and rainfall variability for the 1930–93period. Average characteristics of the rainfall data were explored for 99 stations in that study. Moreover, variations for 91 stations in Turkey, normalized rainfall series, and spatial distribution of the normalized rainfall index were examined. This study showed that given the dry conditions that dominated over the last 20 years, severe and widespread drought events occurred in 1973, 1984, 1989, and 1990. Moreover, winter precipitation had the most distinct values. For many stations, the winter of 1973 happened to be the driest one of the 64-year study scope.

Kömüşçü et al. (2004) applied the standardized precipitation index (SPI), a meteorological index developed by McKee et al. (1993), to research the drought climatology of Turkey. The research intended to study the multi-natural characteristics of the drought with respect to drought frequency in intensity and its spatial extension in order to find drought-prone areas and drought vulnerability. This study revealed that drought events depict a very diverse but consistent picture with changing time scopes such as the occurrence of severe droughts at shorter time periods are typical to the inland of the country.

Tosunoğlu and Can (2016) conducted a research with copulas to model the joint probability distributions of meteorological droughts of Turkey. Monthly precipitation data from 173 gauge stations uniformly distributed across Turkey for the period of 1966–2006 was used. Their findings indicate that drought characteristics were highly correlated and followed various probability distributions. Copula functions were used to build the joint distribution function of drought duration and severity series. The Gamma, Weibull, and generalized Pareto distributions show better fit for the severity series, whereas two-parameter Log-normal distribution is indicated as the best suitable for the duration series.

Dabanlı (2018) utilized the drought hazard index (DHI) formatted on the probability of drought occurrences using the standardized precipitation index (SPI). A total of four socioeconomic indicators were used to quantify drought impact on society and calculate the drought vulnerability index (DVI). Drought risk index (DRI) was calculated by multiplying DHI and DVI for provinces of Turkey to express the relative importance of hazard and vulnerability assessment for drought risk management. The study highlights that 73 are exposed to low, 6 to moderate and only one (Konya) is exposed to high drought risk among 81 administrative provinces.

Present paper revealed the periodical and seasonal meteorological drought conditions in Turkey. The only defect of this study is the use of the SPI method, which is based only on precipitation, among the parameters that constitute the hydrological cycle, because climatic factors are interrelated, and omitting one can mean ignoring for the rest. Nevertheless, the reliability of the findings obtained in this study is unequivocal, since SPI can be calculated easily and there are numerous studies that have been proven to be accurate in

practice. Moreover, the Pearson Type III distribution was used in this study instead of the Gamma distribution, which does not exactly fit the precipitation data (Blain and Meschiatti 2015). Compared to contemporary scholarship, the analysis of seasonal drought in this study deepened the drought knowledge on Turkey. Working in different return periods has increased the support of the study for future climate projections. This is principally valuable in irrigation and water resources management. Seasonal drought studies are particularly momentous in agricultural structures, irrigation, and water planning projects where seasonality is more important. The fact that the study period was quite broad (1925–2016) increased the reliability of the findings obtained in statistical terms. This increases the reliability of trend analysis, which is indispensable especially in hydrological studies.

The results obtained in this paper about drought in Turkey coincide with the previous studies. However, the method used, periodical observation duration, and meteorological precipitation data obtained from different observational points may have caused the general or regional results to be interpreted differently. The increase in drought trend especially in autumn seasons may be a sign of seasonal shifts, because in the Mediterranean Basin, where Turkey is located, the hydrological year starts in the autumn season and the change in this season affects the entire hydrological year. A slight increase in temperatures causes the first frost events expected in autumn to be later. This causes the winter to be shorter and spring to come earlier. This also affects the entire environmental life cycle, causing trees and plants to bloom earlier than normal. Therefore, the most important season in drought assessment can be identified as autumn.

5 Conclusion

Turkey is a country located in the temperate zone of the Northern Hemisphere. Due to the fact that it is surrounded by the sea on 3 sides, the direction of the mountains, and the location above sea level, several climate types can be observed together. While the northeastern part of the country receives abundant rainfall, the eastern end, the southeastern, and central parts receive little rainfall.

This study comprises seasonal drought analyses performed using monthly total rainfall data of 126 observational points spread across Turkey during 1925–2016.

Each season shows different characteristics throughout Turkey in general. It was determined that the autumn season is the driest and spring is the wettest season. Especially in the inner parts of the country, a statistically significant increase in drought was observed during the autumn seasons. There is an insignificant increase in drought generally in Turkey. Theory of Runs suggests that the most intense drought was recorded in autumn seasons. Droughts are becoming severe especially in the southern part of the east of the country. Joint return periods have been examined for conditions ($D \geq 3$ and $S \geq 3$), ($D \geq 3$ or $S \geq 3$), ($D \geq 6$ and $S \geq 6$), ($D \geq 6$ or $S \geq 6$), ($D \geq 9$ and $S \geq 9$), and ($D \geq 9$ or $S \geq 9$). The drought period values found with "and" are higher than those found with "or." According to joint return period data, Turkey is a country where severe drought cases are occurring more frequently. The return periods of 2, 5, 10, 20, 50, and 100 years examined for the ($D \geq 6$ and $S \geq 6$) model showed that the severity of drought increases in the central parts of the country, especially in the 20- and 100-year periods.

There are substantial implications for Turkey in this study. Turkey's southeastern, southern, and central regions are located in a semiarid climate strip, and they are facing desertification risk. Climate change will have a more significant effect, eventually turning the

climate of the southern half of Turkey into a similar climate that of neighboring Syria and Iraq. The climate of central and northern Turkey will be replaced by the current climate of southern Turkey. This means an increased risk of drought and desertification all over the country (Kurnaz 2014).

This study is expected to raise awareness on the water management and water structures projects, basin management studies, agricultural activities, and climatic studies planned to be carried out in Turkey, where climate change is felt concretely.

Author's contributions This study was conceived by Topçu and all of the analysis and drafting of the manuscript was conducted by Topçu.

Funding There is no funding for this research study.

Data availability The data used in this research will not be available.

Declarations

Conflict of interest The author declares that he has no conflict of interest.

Ethical approval There are no ethical issues in this study.

Consent to participate This research has been approved by author and signed on the signature.

Consent for publication The author agrees to the publication of this research and the copyright statement.

References

Addi M, Asare K, Fosuhene KS, Ansah-Narh T, Aidoo K, Botchway GC (2021) Impact of large-scale climate indices on meteorological drought of coastal Ghana. Adv Meteorol 2021:17. https://doi.org/10.1155/2021/8899645

Ahmed K, Shahid S, Harun SB, Wang XJ (2016) Characterization of seasonal droughts in Balochistan Province. Pakistan Stoch Environ Res Risk Assess 30:747–762

Ahmed K, Shahid S, Ismail T, Nawaz N, Wang XJ (2018) Absolute homogeneity assessment of precipitation time series in an arid region of Pakistan. Atmósfera 31(3):301–316

Ahmed K, Shahid S, Sachindra DA, Nawaz N, Chung ES (2019) Fidelity assessment of general circulation model simulated precipitation and temperature over Pakistan using a feature selection method. J Hydrol 573:281–298

An Q, He H, Gao J, Nie Q, Cui Y, Wei C, Xie X (2020) Analysis of temporal-spatial variation characteristics of drought: a case study from Xinjiang China. Water 12:741. https://doi.org/10.3390/w12030741

Blain GC (2011) Standardized Precipitation Index based on Pearson type III distribution. RevistaBrasileira De Meteorologia 26(2):167–180

Blain GC, Meschiatti MC (2015) Inadequacy of the gamma distribution to calculate the Standardized Precipitation Index. RevistaBrasileira De EngenhariaAgrícola e Ambiental 19(12):1129–1135

Cavus Y, Aksoy H (2019) Spatial drought characterization for Seyhan river basin in the Mediterranean region of Turkey. Water 11:1331. https://doi.org/10.3390/w11071331

Chen J, Shi HY, Sivakumar B, Peart MR (2016) Population, water, food, energy and dams. Renew Sustain Energy Rev 56:18–28

Chen L, Singh PV, Guo S (2011) Drought analysis based on copulas. In: 2011 symposium on data-driven approaches to droughts. Paper 45. http://docs.lib.purdue.edu/ddad2011/45

Dabanlı I (2018) Drought hazard, vulnerability, and risk assessment in Turkey. Arab J Geosci 11:538. https://doi.org/10.1007/s12517-018-3867-x

European Commission (2007) European Commission—High level group on science education; European commission—science, economy and society. Science education now: a renewed pedagogy for the

future of Europe; office for official publications of the European communities: Luxembourg, ISBN 927905659X
Farooq M, Wahid A, Kobayashi N, Fujita D, Basra SMA (2009) Plant drought stress: effects, mechanisms and management. In: Sustainable agriculture, Springer: Dordrecht, The Netherlands. https://doi.org/10.1007/978-90-481-2666-8_12
Foster ET, Schmalzer AP, Fox AG (2014) Timing matters: the seasonal effect of drought on tree growth. J Torrey Bot Soc 141(3):225–241
Geiger R (1954) Klassifikation der Klimatenach W. Köppen. In Landolt-Börnstein—Zahlenwerte und FunktionenausPhysik, Chemie, Astronomie, Geophysik und Technik; alte Serie; Springer: Berlin, Germany, Volume 3, pp. 603–607.
Genest C, Favre AC, Béliveau J, Jacques C (2007) Metaelliptical copulas and their use in frequency analysis of multivariate hydrological data. Water Resour Res 43(9):W09401
Guo H, Bao A, Liu T, Ndayisaba F, He D, Kurban A, De Maeyer P (2017) Meteorological drought analysis in the lower Mekong Basin using satellite-based long-term CHIRPS Product. Sustainability 9:901. https://doi.org/10.3390/su9060901
Guofeng Z, Dahe Q, Yuanfeng L, Fenli C, Pengfei H, Dongdong C, Kai W (2017) Accuracy of TRMM precipitation data in the southwest monsoon region of China. Teor Appl Climatol 129(1–2):353–362
Gupta V, Jain MK (2017) Spatio-temporal analysis of trends and periodicities of regional drought projections in India. In: EGU general assembly conference abstracts, 19: 15327
Guttman GB (1999) Accepting the Standardized Precipitation Index: a calculation algorithm Index. J Am Water Resour 35(2):311–322
Hayes M, Wilhite DA, Svoboda M, Vanyarkho O (1999) Monitoring the 1996 drought using standardized precipitation index. Bull Am Meteor Soc 80:429–438
Hosking JRM (1990) L-moments: analysis and estimation of distribution using linear combination of order statistics. J Roy Stat Soc 58(1):105–124
Hosking JRM, Wallis JR (1997) Regional frequency analysis. Cambridge University Press, Cambridge, p 224p
IPCC (2007) IPCC fourth assessment report working Group I report, the physical science basis. Cambridge University Press, New York
IPCC (2014) Climate change 2014: impacts, adaptation, and vulnerability. Contribution of working Group II to the fifth assessment report of the intergovernmental panel on climate change. Cambridge University Press, Cambridge
Irvem A, Ozbuldu M (2019) Evaluation of satellite and reanalysis precipitation products using GIS for all basins in Turkey. Adv Meteorol 2019:11. https://doi.org/10.1155/2019/4820136
Ji L, Peters AJ (2003) Assessing vegetation response to drought in the Northern Great Plains using vegetation and drought indices. Remote Sens Environ 87:85–98
Jones PD, Hulme M, Bria KR, Jones CG (1996) Summer moisture availability over Europe in the Hadley centre general circulation model based on the Palmer drought severity index. Int J Climatol 16:155–172
Júnior RLR, Silva SDF, Costa LR, Gomes BH, Pinto CDD, Herdies LD (2020) Bivariate assessment of drought return periods and frequency in Brazilian Northeast using joint distribution by copula method. Geosciences 10:135. https://doi.org/10.3390/geosciences10040135
Kapluhan E (2013) Türkiye'de Kuraklık ve Kuraklığın Tarıma Etkisi. Marmara Coğrafya Dergisi 27:487–510
Kaptue AT, Hanan NP, Prihodko L, Ramirez JA (2015) Spatial and temporal characteristics of rainfall in Africa: summary statistics for temporal downscaling, Water Resour. Resources 51:2668–2679
Katipoğlu MO, Can I (2018) Estimation Of drought risks using Archimedean copulas in the Karasu River, Turkey. Fresenius Environ Bull 27:9799–9811
Khan N, Shahid S, Juneng L, Ahmed K, Ismail T, Nawaz N (2019) Prediction of heat waves in Pakistan using quantile regression forests. Atmos Res 221:1–11
Komuscu AU (2001) An analysis of recent drought conditions in Turkey in relation to circulation patterns. Drought Network News, Summer–Fall 2001, University of Nebraska Lincoln. Drought-Natl. Drought Mitig. Cent., 13, 5–6
Kömüşçü ÜA, Erkan A, Turgu E, Sönmez KF (2004) A new insight into drought vulnerability in Turkey using the standard precipitation index. J Environ Hydrol 12:18
Kumar VP, Selvam PS, Gitty R (2014) Drought scenario assessment using Standardized Precipitation Index (SPI), international. J Sci Eng Res 5(12)
Kurnaz L (2014) Drought in Turkey, IPC–Mercator Policy Brief, İstanbul Policy Center, SabancıÜniversitesi-İstanbul

Lake PS (2003) Ecological effects of perturbation by drought in flowing waters. Freshw Biol. https://doi.org/10.1046/j.1365-2427.2003.01086.x
Liu S, Shi H, Niu J, Chen J, Kuang X (2020) Assessing future socioeconomic drought events under a changing climate over the Pearl River basin in South China. J Hydrol: Reg Stu 30:100700
Maccioni P, Kossida M, Brocca L, Moramarco T (2015) Assessment of the drought hazard in the Tiber River basin in central Italy and a comparison of new and commonly used meteorological indicators. J Hydrol Eng 20(8):05014029. https://doi.org/10.1061/(asce)he.1943-5584.0001094
Mahajan DR, Dodamani BM (2016) Spatial and temporal drought analysis in the Krishna river basin of Maharashtra. India Cogent Eng 3:1185926
Mancosu N, Snyder RI, Kyriakakis G, Spano D (2015) Water scarcity and future challenges for food production. Water 7(3):975–992
McKee TB, Doesken NJ, Kleist J (1993) The relationship of drought frequency and duration to time scales. In: Proceedings of the 8th conference on applied climatology, Anaheim, 17-22 January 1993, 179-184
Miao CY, Ashouri H, Hsu KL, Sorooshian S, Duan QY (2015) Evaluation of the PERSIANN-CDR daily rainfall estimates in capturing the behavior of extreme precipitation events over china. J Hydrometeorol 16:1387–1396
Mishra AK, Singh VP (2010) A review of drought concepts. J Hydrol 391:202–216
Mishra AK, Singh VP (2011) Drought modeling—A review. J Hydrol 403:157–175
Musonda B, Jing Y, Iyakaremye V, Ojara M (2020) Analysis of long-term variations of drought characteristics using standardized Precipitation Index over Zambia. Atmosphere 11:1268. https://doi.org/10.3390/atmos11121268
Naumann G, Barbosa P, Carrao H, Singleton A (2012) Vogt J (2012) Monitoring drought conditions and their uncertainties in Africa using trmm data. J Appl Meteorol Climatol 51:1867–1874
Petracca M, D'Adderio LP, Porc`u F, Vulpiani G, Sebastianelli S, Puca S (2018) Validation of GPM dual frequency precipitation radar (DPR) rainfall products over Italy, J Hydrometeorol 19(5): 907–925
Qutbudin I, Shiru SM, Sharafati A, Ahmed K, Al-Ansari N, Yaseen MZ, Shahid S, Wang X (2019) Seasonal drought pattern changes due to climate variability: case study in Afghanistan. Water 11:1096. https://doi.org/10.3390/w11051096
Salman SA, Shahid S, Ismail T, Chung ES, Al-Abadi AM (2017) Long-term trends in daily temperature extremes in Iraq. Atmos Res 198:97–107
Salmi T, Maata A, Antilla P, Ruoho-Airola T, Amnell T (2002) Detecting trend of annual values of atmospheric pollutants by the Mann–Kendall test and Sen's slope estimates – the Excel template application Makesens. Finnish Meteorological Institute, Helsinki, Finland, 35 pp
Samarah NH (2005) Effects of drought stress on growth and yield of barley. Agron Sustain Dev 25(1):145–149. https://doi.org/10.1051/agro:2004064
Seckler D, Barker R, Amarasinghe UA (1999) Water scarcity in the twenty-first century. Int J Water Resour Dev 15(1–2):29–42
Şen Z, Almazroui M (2021) Actual Precipitation Index (API) for drought classification. Earth Syst Environ 5:59–70
Serinaldi F, Bonaccorso B, Cancelliere A, Grimaldi S (2009) Probabilistic characterization of drought properties through copulas. Phys Chem Earth Parts A/B/C 34(10–12):596–605
Shi HY, Chen J, Liu SN, Sivakumar B (2019) The role of large dams in promoting economic development under the pressure of population growth. Sustainability 11(10):2965. https://doi.org/10.3390/su11102965
Shiau JT, Shen HW (2001) Recurrence analysis of hydrologic droughts of differing severity. J Water Resour Plan Manag-Asce 127(1):30–40
Shiru MS, Shahid S, Chung ES, Alias N (2019) Changing characteristics of meteorological droughts in Nigeria during 1901–2010. Atmos Res 223:60–73
Singh RG, Jain KM, Gupta V (2019) Spatiotemporal assessment of drought hazard, vulnerability and risk in the Krishna River basin. India, Natural Hazards. https://doi.org/10.1007/s11069-019-03762-6
Sklar A (1959) Fonctions de répartition à n dimensions et leursmarges. Publ Inst Stat Univ Paris 8:229–231
Smirnov O, Zhang MH, Xiao TY, Orbell J, Lobben A, Gordon J (2016) The relative importance of climate change and population growth for exposure to future extreme droughts. Clim Change 138(1–2):41–53
Sonmez FK, Komuscu AU, Erkan A, Turgu E (2005) An analysis of spatial and temporal dimension of drought vulnerability in Turkey using the standardized precipitation index. Nat Hazard 35:243–264
Spinoni J, Naumann G, Carrão H, Barbosa P, Vogt J (2014) World drought frequency, duration, and severity for 1951–2010. Int J Climatol 34:2792–2804
Topçu E, Seçkin N (2016) Drought analysis of the Seyhan Basin by using Standardized Precipitation Index (SPI) and L-moments. J Agri Sci 22:196–215

Tosunoğlu F, Can I (2016) Application of copulas for regional bivariate frequency analysis of meteorological droughts in Turkey. Nat Hazards. https://doi.org/10.1007/s11069-016-2253-9
Trenberth KE, Dai A, Van Der Schrier G, Jones PD, Barichivich J, Bria KR, Sheeld J (2014) Global warming and changes in drought. Nat Clim Chang 4:17–22
Trinh T, Ishida K, Kavvas ML, Ercan A, Carr K (2017) Assessment of 21st century drought conditions at Shasta Dam based on dynamically projected water supply conditions by a regional climate model coupled with a physically-based hydrology model. Sci Total Environ 586:197–205
Turkes M (1996) Spatial and temporal analysis of annual rainfall variations in Turkey. Int J Climatol 16:1057–1076
Vicente-Serrano SM, Begueria S (2006) Differences in spatial patterns of drought on different time scales: an analysis of the Iberian peninsula. Water Resour Manag 20:37–60
Wang R, Zhao C, Zhang J, Guo E, Li D, Alu S, Ha S, Dong Z (2018) Bivariate copula function-based spatial-temporal characteristics analysis of drought in Anhui Province. China Meteorol Atmos Phys 131:1341–1355
Wilhite DA, Glantz MH (1985) Understanding: the drought phenomenon: the role of definitions. Water Int 10(3):111–120
Wilhite DA, Sivakumar MVK, Pulwarty R (2014) Managing drought risk in a changing climate: the role of national drought policy. Weather Clim Extrem 3:4–13
Wilhite DA, Svoboda MD, Hayes MJ (2007) Understanding the complex impacts of drought: a key to enhancing drought mitigation and preparedness. Water Resour Manag 21:763–774
World Bank Climate change knowledge portal, Download Data (2021), https://climateknowledgeportal.worldbank.org/download-data (05.04.2021).
Yevjevich VM (1967) An objective approach to definitions and investigations of continental hydrologic droughts. Hydrology Papers Colorado State University Fort Collins, Colorado, No 23
Yu M, Li Q, Hayes MJ, Svoboda MD, Heim RR (2014) Are droughts becoming more frequent or severe in China based on the standardized precipitation evapotranspiration index: 1951–2010? Int J Climatol 34:545–558
Zhu Q, Xuan W, Liu L, Xu YP (2016) Evaluation and hydrological application of precipitation estimates derived from PERSIANN-CDR, TRMM 3B42V7, and NCEP-CFSR over humid regions in China. Hydrol Process 30(17):3061–3083

Publisher's Note Springer Nature remains neutral with regard to jurisdictional claims in published maps and institutional affiliations.